

# Low Cost, Tiny Sized MEMS Hydrophone Sensor For Water Pipeline Leak Detection

Jinghui Xu, Kevin Tshun-Chuan Chai, Member, IEEE, Guoqiang Wu, Beibei Han, Eva Leong-Ching Wai, Wei Li, Jason Yeo, Edwin Nijhof, and Yuandong Gu

**Abstract**—In this paper, we present an experimental investigation of a water pipeline leak detection system based on a low cost, tiny sized hydrophone sensor fabricated using the micro-electro-mechanical system (MEMS) technologies. A  $10 \times 10$  element arrayed MEMS hydrophone device with chip size of  $3.5 \times 3.5$  mm $^2$  was used in the experiment. The hydrophone device is packaged with a customized on-board pre-amplification circuit using an acoustic transparent material. The overall package size of the MEMS hydrophone is  $\Phi 1.2$  cm  $\times$  2.5 cm. The packaged MEMS hydrophone achieves an acoustic sensitivity of -180 dB (re: 1 V/ $\mu$ Pa), a bandwidth from 10 Hz to 8 kHz, and a noise resolution of around 60 dB (re: 1  $\mu$ Pa/ $\sqrt{Hz}$ ) at 1 kHz. A section of ductile iron water pipeline with an internal diameter of 10 cm, wall thickness of 0.73 cm and length of 30 m is constructed as the test bed for the water leak detection. Two different leak sizes with leak flow rates of about 30 L/min and 180 L/min are designed along the pipe, which is pressurized at 3.2 Bar. Analysis of the transient signals and spectrograms shows that the MEMS hydrophone can capture the key acoustic information of the water leak, i.e. identifying the leak and locating the leak position. The measurement results demonstrate the feasibility to construct an affordable, highly efficient, real-time, and permanent in-pipe pipeline health monitoring networks based on the MEMS hydrophones due to their high performance, low cost and tiny size.

**Index Terms**—Micro-electro-mechanical systems (MEMS), AlN, Hydrophone, Ultrasonic sensor, Pipeline, Leak detection.

## I. INTRODUCTION

SUFFICIENT water supply is crucial for sustainable economic activities and our daily lives. A large portion of water is lost during transportation and distribution, commonly known as non-revenue water (NRW). It is reported that the NRWs of most of the large cities in the developing countries and a lot of old cities in the developed countries are above 30% in 2011, it is even higher than 50% in some cities, such as

This work is part of MEMS Technology commercialization project supported by Exploit Technologies Pte. Ltd. (ETPL), and JCS Venture Lab, the corporate incubator of JCS Group, Singapore. (J. Xu, K. T.-C. Chai and G. Wu contributed equally to this work.) (Corresponding author: Y. Gu.)

J. Xu, K. T.-C. Chai, G. Wu, B. Han, E. L.-C. Wai and Y. Gu are with Institute of Microelectronics, Agency for Science, Technology and Research (A\*STAR), 2 Fusionopolis Way, #08-02, Innovis, Singapore, 138634. J. Xu is also with MEMSound Pte. Ltd, Singapore. (e-mail: xuj@ime.a-star.edu.sg, chaitc@ime.a-star.edu.sg, wugq@ime.a-star.edu.sg, hanb@ime.a-star.edu.sg, wail@ime.a-star.edu.sg and guyd@ime.a-star.edu.sg)

W. Li is with Exploit Technologies Pte. Ltd. (ETPL), Agency for Science, Technology and Research (A\*STAR), Singapore. He is also with JCS Group, Singapore. (e-mail: Li\_Wei@etpl.sg)

J. Yeo and E. Nijhof are with JCS Group, Singapore. (email: jason@jcsauto.com.sg and edwin@jcstech.com.sg)

Jakarta, Delhi, Adana etc. [1]–[4]. Although the NRW indicator has decreased in the past 5 years since the leak detection systems are gradually adopted, the NRW indicators are still above 30%. In 2016, the World Bank reported that roughly 45 million cubic meters of water are lost daily in developing countries, an amount of which is sufficient to supply 200 million people or worth an economic value of over USD 3 billion per year [5]. What exacerbates the problem is that the countries with serious water loss are usually those which lack water resource. The World Bank also puts the global estimate of physical water losses at 32 billion cubic meters each year, twice of that occurring in developing countries.

The NRW is attributed to a variety of sources, including metering errors, accounting errors, water theft and pipeline leakage. The water loss due to pipeline leak is as high as 30% of the total flow, which is the main component of the water loss [6]–[9]. Water pipelines are mainly classified into two categories, namely distribution pipelines and transmission pipelines. The leak in the transmission pipeline is usually caused by the cracks. This kind of leak can be found immediately since the cracks will suddenly induce the large variations of the water supply pressures, which can be quickly alarmed by the pressure meters. It is reported that more than 80% of the water leak through pipeline is from the distribution pipeline. Therefore, efficient pipeline leak detection is the only viable long-term solution, and over the last two decades it has been widely studied.

There are two systematic leakage-control programs [9]–[14]. One is water audits and the other is leak-detection surveys. Although water audit gives a good indication of the amount of wafer losses, it provides no information about the locations of these losses. Leak-detection surveys are able to determine the exact location of the leaks using acoustic or non-acoustic techniques. Listening rods, aquaphones, and ground microphones are used to pinpoint the leak by listening on all accessible contact points with the distribution system. As another option, suspected pipeline leaks can be pinpointed automatically by using modern acoustic correlators. In this method, the suspected leak is detected by two hydrophones and the time lag between the received acoustic signals acquired by hydrophones is used to identify location of the leak. Besides the above two acoustic detection approaches, several non-acoustic techniques such as pressure transient, tracer gas, infrared imaging and satellite scanning could be also used to detect the pipeline leaks [9], [10]. However, these non-acoustic techniques are still very limited and not as effective as the

well-established acoustic approaches.

Among the leak detection techniques, the acoustic correlator method has been increasingly used because it is more efficient and accurate than the listening devices. The acoustic correlator approach requires two hydrophones to measure the acoustic signals. However, the existing piezoceramic-based hydrophones suffer from large size, high cost and high power consumption.

Recently, permanent acoustic sensor networks are proposed for real-time pipeline health monitoring [15]–[17]. The networks required a large number of hydrophone sensors to be installed inside the pipeline for reducing the influence the external environmental noise. Therefore, there is a strong need for a low cost and compact size hydrophone sensors, in order to construct an affordable sensor network for the real-time leak detections of the pipelines. In this work, a feasibility study of leak detection is performed by using the micro-electromechanical system (MEMS) hydrophones, which feature compact size, low cost and small power consumption. The reported MEMS hydrophones exhibit great potential applications in the pipeline leak detection networks.

This paper presents an experimental investigation of a water pipeline leak detection, for the first time, using a low cost, tiny sized hydrophone sensor based on MEMS technology. The fabrication, packaging and characterization of the MEMS hydrophone sensor are described in section II. The experiment setup for the pipeline leak detection is illustrated in section III. The experiment results and detailed analysis are reported in section IV. Section V reported the evaluation of reliability and long-term stability of the reported MEMS hydrophones and finally section VI concludes the paper.

## II. MEMS HYDROPHONE

The reported MEMS hydrophone sensor is fabricated based on an 8-inch CMOS-compatible piezoelectric integration platform. The hydrophone consists of a cavity-SOI wafer with a sandwiched piezoelectric layer of Molybdenum-Aluminum Nitride-Molybdenum (Mo-AlN-Mo) on top of it [18]. A sandwiched piezoelectric is used to sense the acoustic signals caused by the water leak in the pipeline [19]. Fig. 1(a) shows the cross-sectional view of the fabricated piezoelectric Mo-AlN-Mo stack. The sputtered AlN thin film is fully c-axis oriented with a full width at half maximum (FWHM) value of  $1.39^\circ$ , which is obtained from the X-ray diffraction (XRD) rocking curve as shown in Fig. 1(b) [20]. Fig. 2(a) shows a scanning electron microscopy (SEM) image of the fabricated  $10 \times 10$  elements device, and Fig. 2(b) shows the zoomed in view of each element which clearly indicates the membrane structure and electrical connections. The dimension of the fabricated  $10 \times 10$  hydrophone chip is about  $3.5 \times 3.5$  mm $^2$ , which is much smaller than the traditional piezo-ceramic hydrophone counterparts by one order of magnitude [21].

A customized signal conditioning and amplification read-out circuit is designed to pick up the electrical charges generated by the MEMS hydrophone during operation. Fig. 3 shows the schematic diagram of a voltage-mode amplification circuit used in our work. The circuit is designed to have a gain of

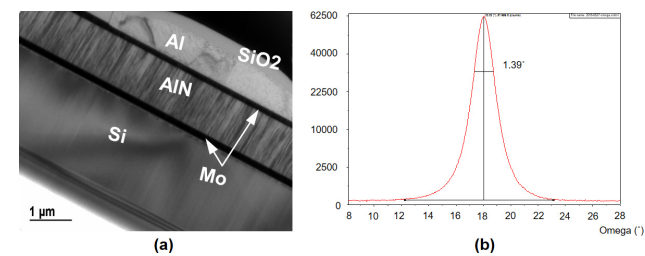


Fig. 1. Fabricated Mo-AlN-Mo piezoelectric stack. (a) SEM image showing the excellent crystal orientation, and (b) the measured XRD texture of the AlN film with FWHM value of  $1.39^\circ$ .

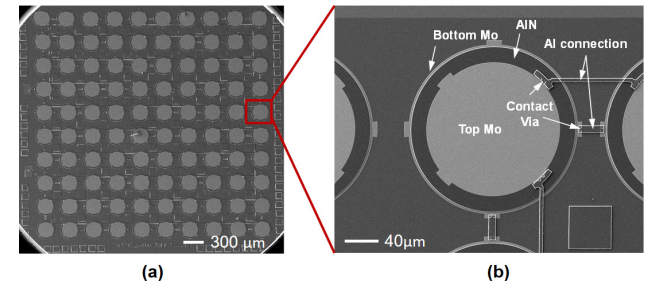


Fig. 2. Fabricated MEMS hydrophone device. (a)  $10 \times 10$  device with chip size  $3.5 \times 3.5$  mm $^2$ , and (b) zoomed in view showing the electrical connection

40 dB and feature a flat response from 10 Hz to 10 kHz. The voltage output ( $V_o$ ), lower cut-off frequency  $f_L$  and upper cut-off frequency  $f_H$  are given by the following equations [22]:

$$\begin{aligned} V_o &= \frac{V_{dd}}{2} + \frac{Q_0}{C_0 + C_p} \times \left(1 + \frac{R_f}{R_g}\right) \\ f_L &= \frac{R_0 + R_b}{2\pi(R_0 \times R_b)(C_0 + C_p)} \\ f_H &= \frac{1}{2\pi R_f C_f} \end{aligned} \quad (1)$$

where

$Q_0$  = charge generated by the MEMS hydrophone

$C_0$  = initial capacitance of the MEMS hydrophone

$R_0$  = device DC-resistance

$C_p$  = parasitic capacitances

$R_f$  = feedback resistance

$C_f$  = feedback capacitance

$R_g$  = gain resistance

$R_b$  = DC filter resistance

$V_{dd}$  = supply DC voltage.

It is reported that the sound signal emitted by pipeline leak contains a very low frequency (around 10 Hz) component [23], [24]. Therefore, the bandwidth of the circuit must be extended to a low enough frequency range in order to capture the leak signal efficiently. To achieve this objective,  $R_0$ ,  $R_b$ ,  $C_0$ ,  $C_p$  should be as large as possible according to Eq. (1). The DC-resistance  $R_0$  usually is huge ( $> 10$  GΩ), which can be ignored and assumed to be an open circuit. The parasitic capacitance  $C_p$  cannot be too high since a large  $C_p$  will decrease the output signal. A large DC resistor  $R_b$  can be purchased off-the-shelf. Therefore, to achieve a low cut-off frequency, the initial capacitance of hydrophone  $C_0$  should be as large as

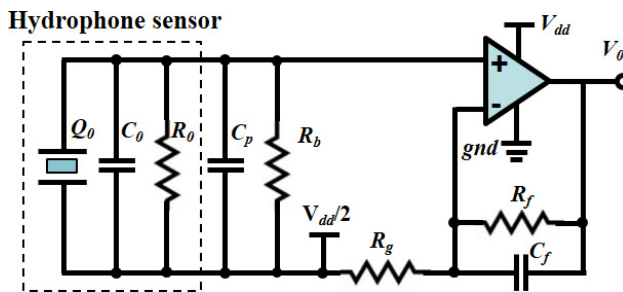


Fig. 3. Schematic diagram of a voltage mode amplification circuit.

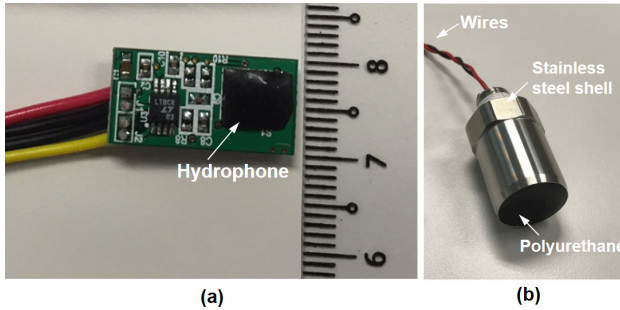


Fig. 4. Hydrophone assembly and packaging. (a) The MEMS hydrophone chip is attached on a PCB. The MEMS chip and bonded wires are protected using an acoustically transparent polyurethane material, and (b) the PCB with MEMS hydrophone is potted into a stainless steel shell using the same polyurethane material.

possible. A  $10 \times 10$  arrayed hydrophone device with  $C_0$  as large as 340 pF is chosen in this work.

Fig. 4 shows an assembled MEMS hydrophone chip on the printed circuit board (PCB), where the hydrophone chip and bonded wires are protected by an acoustically transparent polyurethane film. The assembled PCB is then potted into a stainless steel shell using the same polyurethane material. The final packaged hydrophone is shown in Fig. 4(b), which has a size of  $\Phi 1.2\text{ cm} \times 2.5\text{ cm}$ . It should be noted that a commercial steel shell container is used for testing purpose. The packaged hydrophone size can be further reduced significantly by using a customized container and an application-specific integrated circuit (ASIC) instead of the PCB.

The packaged MEMS hydrophone is characterized with a standard anechoic water pool in a national lab using the Brüel & Kjær Type 8103 hydrophone as the reference. The frequency response measurement results show that the packaged MEMS hydrophone has a very flat response with a sensitivity of  $-180\text{ dB} \pm 1\text{ dB}$  (re:  $1\text{ V}/\mu\text{Pa}$ ) over the bandwidth of 10 Hz to 8 kHz. The noise sources of the MEMS hydrophone limit the detectable acoustic pressure. There main noise sources of the MEMS hydrophone in our work are:  $\tan\delta$  noise or the dielectric loss, input noise voltage of the preamplifier, input noise current of the preamplifier, and the Johnson (thermal) noise. The frequency response of the resulting voltage noise density of a typical MEMS hydrophone is illustrated in Fig. 5. Johnson noise of the high-megohm resistor dominates at a large frequency range (up to 400 Hz). At medium frequencies (400 Hz to 1 kHz),  $\tan\delta$  noise, voltage noise and Johnson noise dominate the resultant noise density. At high frequencies

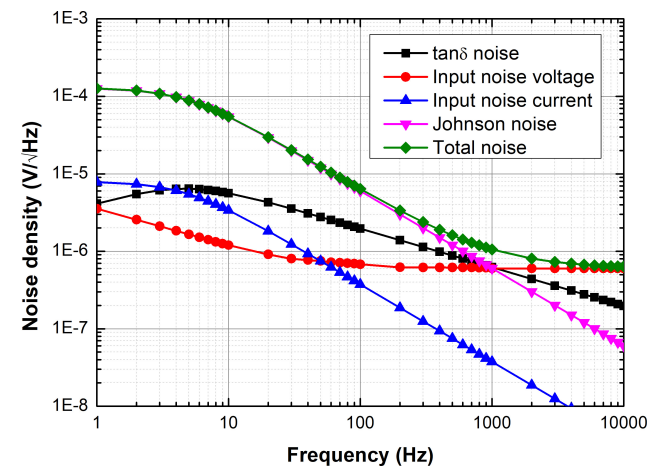


Fig. 5. Frequency response of the resulting voltage noise density of a typical MEMS hydrophone.

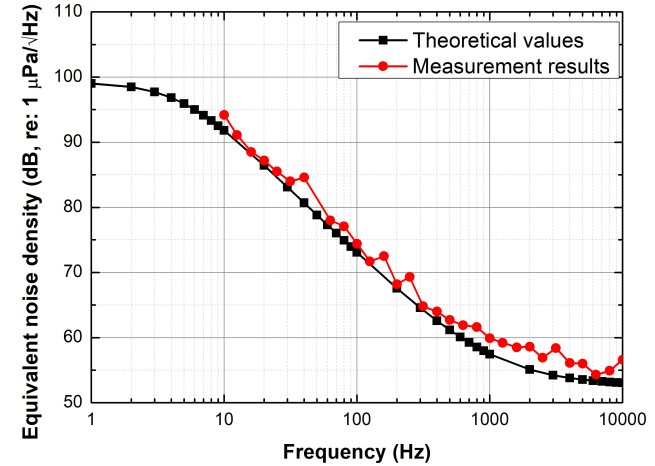


Fig. 6. Comparison of measured and theoretical equivalent pressure noise density of the MEMS hydrophone.

( $> 1\text{ kHz}$ ), the voltage noise of the preamplifier specifies the resultant voltage noise density.

Fig. 6 shows the comparison of measured and theoretical equivalent acoustic pressure noise density of the MEMS hydrophone. The measured equivalent pressure noise densities are in good agreement with the theoretical values. The MEMS hydrophone shows an output noise resolution about 60 dB (re:  $1\text{ }\mu\text{Pa}/\sqrt{\text{Hz}}$ ) at 1 kHz. A comparison of the performance of the developed MEMS hydrophone with the state-of-art commercially available hydrophones is illustrated in Table I. The reported MEMS hydrophone is shown to be a competitive high-performance device compared with the commercial hydrophones.

### III. EXPERIMENT SETUP

It is reported that the water leakage is mainly from the distribution pipeline instead of the transmission pipeline. Therefore, in this paper the experimental study is conducted with a purpose-built pipeline, which is with the same dimension as a typical neighborhood distribution pipeline with internal diameter of 10 cm and wall thickness of 0.73 cm. A 30 m long,

TABLE I  
PERFORMANCE COMPARISON OF THE DEVELOPED MEMS HYDROPHONE WITH THE COMMERCIALLY AVAILABLE HYDROPHONES

Hydrophone	Brüel & Kjær 8103 [25]	Benthowave BII-7152 [26]	DolphinEar DE200 [27]	Aquarian H2a [28]	This work
Technology	Piezoceramic	Piezoceramic	Piezoceramic	Piezoceramic	MEMS Piezoelectric
Sound sensitivity (dB, re: 1 V/ $\mu$ Pa)	-211 ± 2	-196 ± 2	-209 ± 1.5	-180 ± 4	-180 ± 1
Bandwidth (Hz)	3 - 20000	1 - 20000	7 - 22000	20 - 4000	10 - 8000
Noise resolution (dB, re: 1 $\mu$ Pa/ $\sqrt$ Hz)	55 at 1 kHz	~ 50	75	~ 80	60 at 1 kHz
Size	Φ0.9 cm × 5 cm	Φ4.2 cm × 2.5 cm	Φ6 cm × 0.75 cm	Φ2.5 cm × 4.6 cm	Φ1.2 cm × 2.5 cm
Power consumption (mW)	N.A.	12	63	N.A.	5

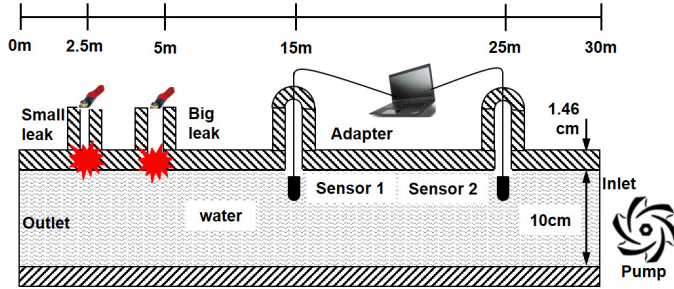


Fig. 7. The schematic diagram of the pipeline and measurement setup. There are two valves for water leak mimic with flow rate of 30 L/min and 180 L/min, respectively. Two packaged MEMS hydrophones are installed in the pipeline using the customized adapters. The sound signals detected by the hydrophones are collected by a laptop for signal analysis and processing.

ductile iron pipe is constructed based on the design schematic as shown in Fig. 7. The pipeline is divided into 5 sections. The locations of the mimic leak holes and hydrophone installation holes (adapters) are illustrated in Fig. 7. The leak holes and hydrophone installation holes can be exchanged for different testing purposes.

These sections are connected using the customized bolts and nuts. A mechanical pump is installed in the inlet which could pump the water and make the supply pressure up to 4 Bar. This is consistent with the real municipal water distribution pressure of most of the cities globally. A pressure meter is added in the loop to monitor the real-time water pressure. The flow rate of the small and big leak are maintained at 30 L/min and 180 L/min respectively while the water supply pressure is maintained at 3.2 Bar during the testing. The packaged MEMS hydrophones are installed into the pipeline using the customized adapters.

In an event of leak, a friction noise will be generated and propagates along the water column and the pipeline. During the experiment, these mimic leak events are captured by the MEMS hydrophone and the signals are transmitted to a laptop for subsequent signal analysis and processing. Fig. 8 shows the assembled pipeline leak detection testing bed installed in a warehouse.

#### IV. RESULTS AND DISCUSSIONS

The MEMS hydrophones are installed inside the pipeline as illustrated in Fig. 7. During the experiment, the water supply pressure is kept at 3.2 Bar. The small leak (valve 1) and big leak (valve 2) are opened and closed based on the following

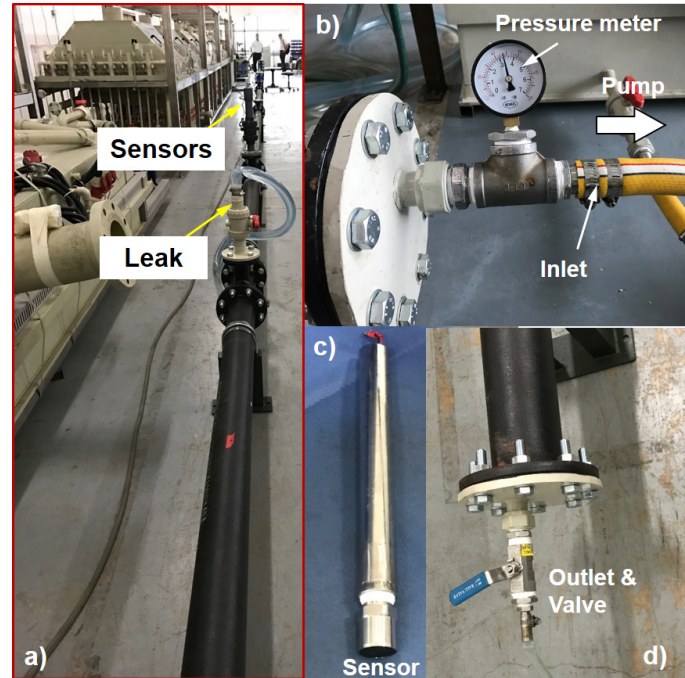


Fig. 8. The assembled pipeline leak measurement setup. (a) The assembled pipeline water leak measurement system, (b) The inlet of the pipeline with a pressure meter and a water pump, (c) The customized adapter with the packaged MEMS hydrophone, and (d) The outlet of the pipeline for water cycling.

sequence: (a) open valve 1, (b) open valve 2, (c) close valve 2, (d) close valve 1, (e) open valve 2, (f) open valve 1, (g) close valve 1, and (h) close valve 2.

#### A. Water Leak Detection

In order to obtain a stable result of each sequence, the two adjacent steps are separated in the time-domain. After getting a stable result causing by the current sequence, the next sequence is triggered. The overall water leak measurement takes about 5 minutes and the captured time-domain signals are presented in Fig. 9, where the environmental vibration noise is removed by signal processing. Fig. 10 shows the spectrogram of the result of Fig. 9. Color in red indicates the highest signal power spectral density (PSD) and the color in blue indicates the lowest PSD in the spectrogram.

Based on the measurement results as shown in Fig. 9 and Fig. 10, it may be concluded that:

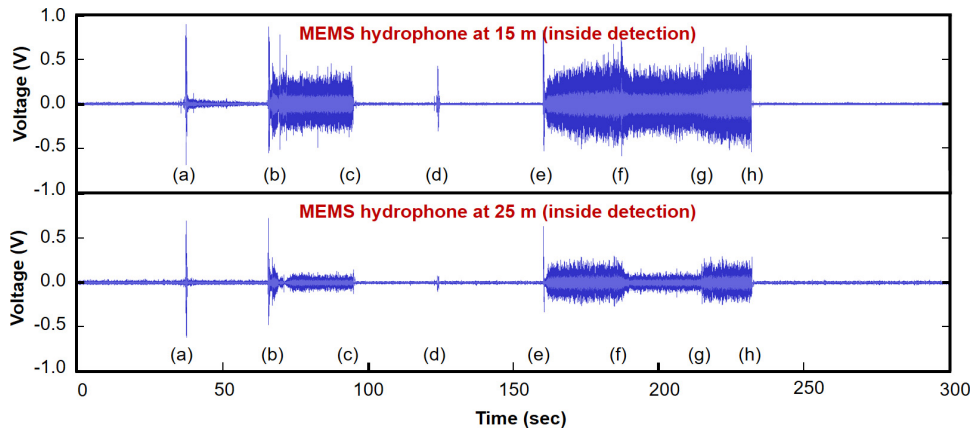


Fig. 9. The time-domain measurement results of the water pipeline leak system using the leak opening and closing sequence (a)-(h).

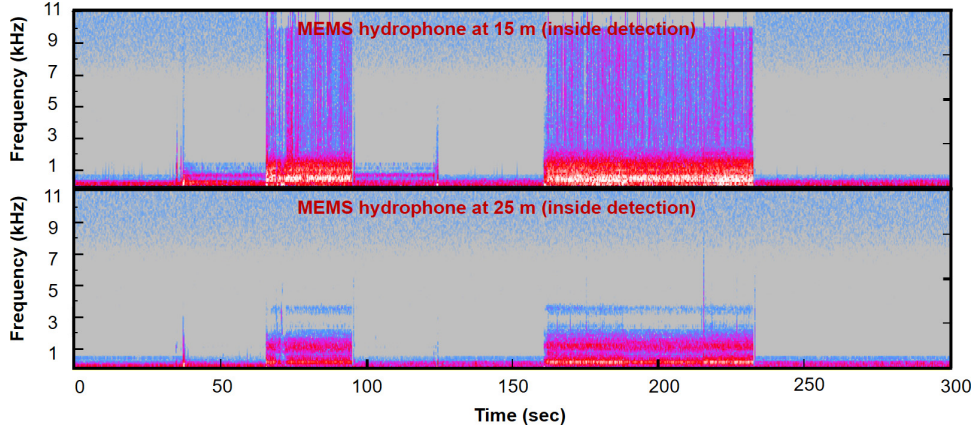


Fig. 10. The signal historical spectrogram of the MEMS hydrophones located at (a) 15 m and (b) 25 m, respectively. Color in red indicates the highest PSD and the color in blue indicates the lowest PSD.

(a) A transient acoustic pulse signal is detected each time a mimic leak occurs;

(b) Both the small and big leaks can be detected by the MEMS hydrophones at different locations. The output voltage of the MEMS hydrophone at 15 m is about 2 times larger than that of the MEMS hydrophone at 25 m. This is to say, there is roughly a 0.6 dB/m transmission loss when assuming the loss is linear with the propagated distance;

(c) The output voltage of the MEMS hydrophone at 15 m is  $\pm 300$  mV when only valve 2 is opened. It indicates that about 300 Pa acoustic pressure is emitted at the location which is 10 m away from the water leak;

(d) Both the existing leak and new leak can be detected. As shown in Fig. 9, the initiation of a leak is received by both MEMS hydrophones as a pulse signal. This pulse signal can be used as a indicator of a new leak. As the leak continues, the MEMS hydrophones continuously receive the emitted acoustic signals. It illustrated that the existing leak can also be detected by the MEMS hydrophones. Both the existing and new leak detections are important, because both of these leak identifications are key missions in the pipeline leak detection;

(e) The spectrograms of the signals indicate that the frequency of the acoustic signals emitted by the leak can be divided into three sub-bands. Firstly, the frequency range up

to 200 Hz corresponds to the longitudinal resonance frequency of the pipe, since longitudinal resonance of the pipe always exists regardless of whether a leakage is present. Secondly, the pipeline leak signals mainly concentrate in the frequency range of 200 Hz to 2 kHz. Finally, the signals with frequency above 2 kHz might be caused by the ambient noises such as vehicular motions and running machinery. The power of the signals beyond 2 kHz will decrease rapidly.

As a stress-sensitive device, the hydrophone responses to all the sound signals, including the leak and external environmental noises. Therefore, it is impossible for hydrophone to decouple the leak signals and the external noises with similar frequencies. However, the leak signals have featured characteristics in frequency domain, which could be analyzed with signal processing schemes. Therefore, signal processing or machine learning-based artificial intelligence (AI) could be an effective way to analysis the receiving signals from the hydrophone and identify the leak signals.

#### B. Comparison of The Inside and Outside Detection Approaches

To implement the leak detection, the installation of the MEMS hydrophones outside the pipeline is preferred, since it is much easier to install, repair or maintain the detection

TABLE II  
THE ACOUSTIC PROPERTIES OF MATERIALS IN USE.

Material	Ductile iron	Polyurethane
Sound speed (m/s)	2650	1450
Density (kg/m <sup>3</sup> )	7300	1000
Acoustic impedance (kg/(m <sup>2</sup> ·s)×10 <sup>6</sup> )	19.35	1.45

systems from the outside than inside. However, the iron pipe may degrade the acoustic signal and the environmental noise may also degrade the accuracy of the leak detections. In order to investigate the feasibility of the wafer leak detection based on the reported MEMS hydrophone using the outside detection approach, measurements with the MEMS hydrophones installed outside the pipeline are conducted.

For the outside detection approach, the MEMS hydrophones are adhered to the pipeline surface tightly. The opening and closing of valves followed the same sequence as that in the previous inside detection approach. The measurement results are recorded and compared with the results of the inside detection approach. Fig. 11 shows the comparison of the measurement results from the MEMS hydrophone located at 15 m between the inside and outside detection approaches.

It can be observed that the signals captured using the two detection approaches show excellent correlation. The signal profile using the outside detection approach almost are the same with that using the inside detection approach. Only the magnitudes are significantly different. There is an around 30 dB signal attenuation using the outside detection approach. One of the main sources of this large attenuation is the acoustic impedance mismatch at the interface between the pipeline and the MEMS hydrophone. Hence, only a small portion of acoustic power is transmitted from the pipeline to the MEMS hydrophone attached on the surface of the pipeline. Table II lists the material properties of the ductile iron used for the pipeline and the polyurethane covered on the hydrophone chip. Assuming the incident sound signal is normal to the interface, the transmitted sound pressure coefficient  $T_p$  can be calculated as follows [29]:

$$T_p = \frac{2Z_2}{Z_1 + Z_2} = \frac{2\rho_2 V_2}{\rho_1 V_1 + \rho_2 V_2} \quad (2)$$

where  $Z_1$  and  $Z_2$ ,  $\rho_1$  and  $\rho_2$ ,  $V_1$  and  $V_2$  are the acoustic impedances, mass densities, and sound speeds of medium 1 and 2, respectively.

Substituting the related material properties into Eq. (2), we obtain  $T_p \approx 0.14$ . In other words, there is a direct 17 dB signal attenuation when the sound signal propagate from ductile iron to the MEMS hydrophone sensor. The remaining 13 dB signal attenuation may be caused by the transmission loss since the sound propagation from inside to outside the pipe is not an ideal plane wave.

Different sensor installation positions away from leak position are investigated and they show similar signal attenuation. It should be noted that the length of each section of the real water distribution pipeline is about 100 m. Assuming a MEMS hydrophone is installed at each junction, the maximum transmission loss of the inside and outside detection approaches

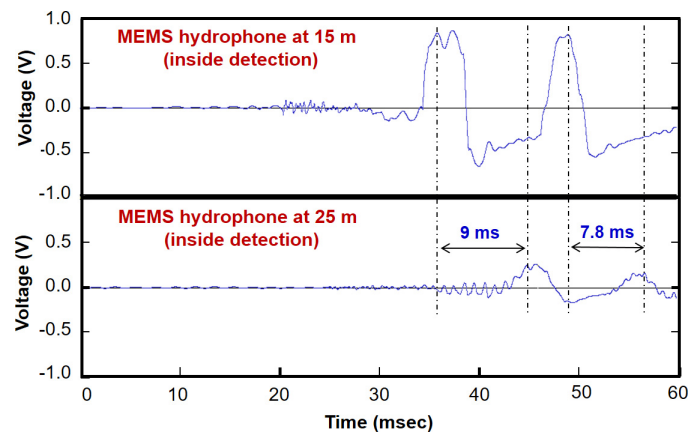


Fig. 12. The correlation results of the measured output signals from the two MEMS hydrophones. It shows that the two signals have very similar profile while there is time delay between the two signals.

will be about 60 dB and 90 dB, respectively. This huge loss will severely affect the signal fidelity and cause potential false alarms. Therefore, the inside detection approach is better in terms of the signal fidelity.

### C. Leak Positioning Evaluation

Besides identifying the leak, another key task of pipeline leak detection system is to ascertain the leak location. This is usually realized by using multi-sensor correlation [30]. In this paper, we performed the leak positioning testing using the two deployed MEMS hydrophones as illustrated in Fig. 7. The output signals from the two MEMS hydrophones are synchronized to the same data acquisition software. From the correlation results of the measured data as shown in Fig. 12, it is observed that both MEMS hydrophones capture similar signal profile while there is a time delay between the two signals. This is because the acoustic signal travels different distances before it arrives at the two MEMS hydrophones. The sound speed in the pipeline can be deduced as:

$$v_s = \frac{d}{\Delta t} \quad (3)$$

where  $v_s$  is the sound speed in water, and  $d = 10$  m is the distance between the two MEMS hydrophones. Assuming  $\Delta t = 9$  ms is the time delay between the received signals from the two MEMS hydrophones, according to Eq. (3), the sound speed in water is calculated to be 1111 m/s. The calculated sound speed is lower than the theoretical value of 1450 m/s by 23.4%, which may be caused by the setup imperfection, such as synchronization error of the two signals. In addition, the sound speed in the water filled in the pipeline is highly dependent on the pipeline material, dimension and the amount of the air bubbles inside the water [29].

In this work, both of the MEMS hydrophones are located at the same side of the leak position. Therefore, this leak detection configuration cannot be used to ascertain the leak location. However, the experiment clearly demonstrates the signal delay, hence proving that leak positioning using the report MEMS hydrophones is feasible.

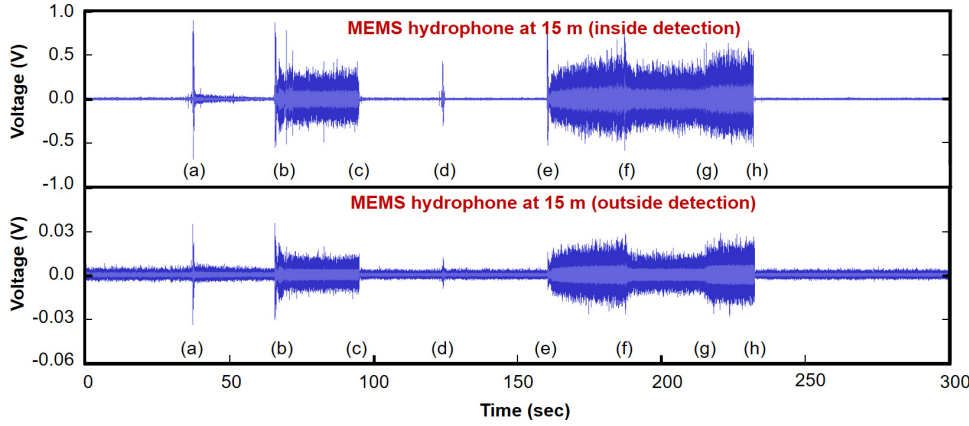


Fig. 11. Comparison of the output voltages from the MEMS hydrophone located at 15 m using the inside and outside detection approaches. It shows that these two approaches have very similar signal profile. While there is about 30 dB signal attenuation using the outside detection approach.

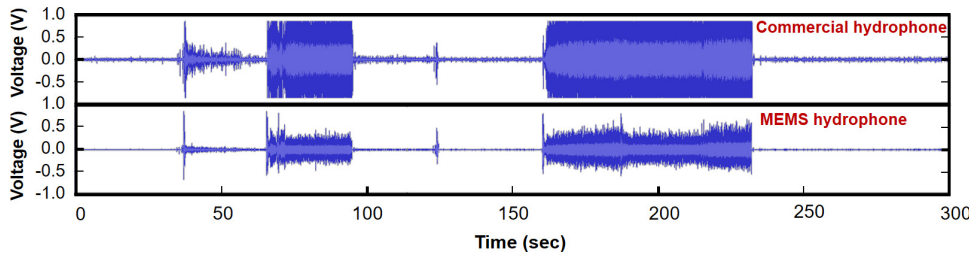


Fig. 13. Comparison of the output voltages from the MEMS hydrophone and the commercial hydrophone. Both of the hydrophone sensors are located at 15 m away from the leak and using the inside detection approach. The two hydrophones have very similar signal profile.

#### D. Comparison With The Commercial Hydrophone

In our work, a commercial piezo-ceramic hydrophone H2a, from Aquarian Audio & Scientific<sup>TM</sup>, is used as the reference hydrophone. This commercial hydrophone is currently used for pipeline leak detection by some industry players. The reference hydrophone is installed at 15 m away from the leak together with the MEMS hydrophone. Fig. 13 shows the comparison of the output voltages from the MEMS hydrophone and the reference hydrophone. Both the reference hydrophone and the MEMS hydrophone capture very similar signal profiles but different signal magnitudes due to different acoustic sensitivities. The experimental result verifies the feasibility of the MEMS hydrophone for the pipeline leak detection, which featuring smaller size, lower cost and decent performance than the commercial piezo-ceramic hydrophone.

#### V. EVALUATION OF RELIABILITY AND LONG-TERM STABILITY

The packaged MEMS hydrophones are evaluated by the high-temperature storage (HTS), low-temperature storage (LTS), and temperature cycling (TC) tests in order to assess the reliability of the packaged devices. Fig. 14 shows the measured sensitivity variations of 5 packaged MEMS hydrophones after the HTS, LTS, and TC tests. The sensitivity drifts of all the 5 hydrophones are less than  $\pm 0.5$  dB ( $\pm 0.56\%$ ). No significant performance drift or failure mechanism is observed after the reliability tests. These measured reliability evaluation results verify the reliability and robustness of the MEMS hydrophones and the packaging. The estimated life time of the packaged

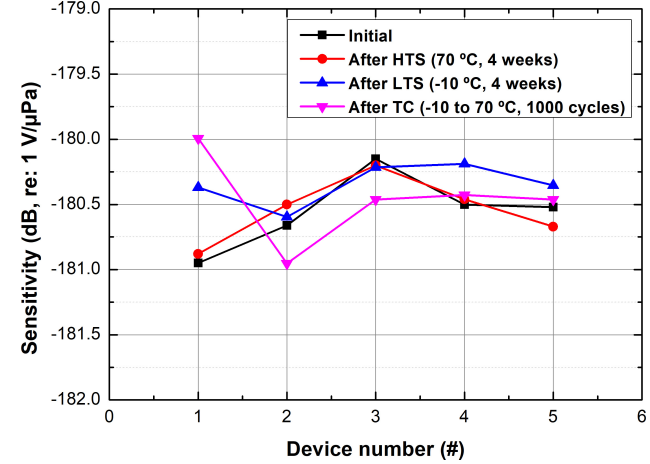


Fig. 14. Reliability tests of 5 packaged hydrophones. The tested hydrophones are evaluated by HTS, LTS, and TC tests, respectively.

MEMS hydrophone is 10.4 years based on the Coffin-Manson model.

The long-term stability measurements have been performed on the MEMS hydrophone, in order to investigate the stability of the packaged MEMS hydrophone over time. Fig. 15 shows the measured sensitivity drifts of a packaged MEMS hydrophone over 1200 days. The sensitivity drift is less than  $\pm 0.3$  dB ( $\pm 0.15\%$ ). The measurement results illustrate that the MEMS hydrophone has excellent long-term stability.

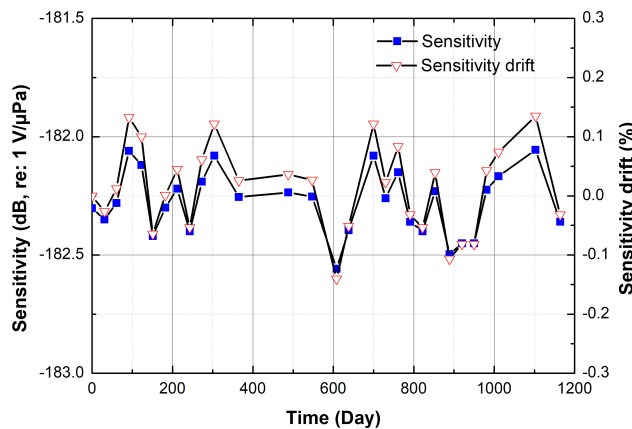


Fig. 15. Long-term stability measurements for the packaged MEMS hydrophone.

## VI. CONCLUSION

This paper experimentally presents a water pipeline leak detection system, for the first time, using a low cost, tiny sized MEMS hydrophone sensor. All the experiments are conducted based on ductile iron pipeline with internal diameter of 10 cm and wall thickness of 0.73 cm. The experiment results indicate that both new and existing leaks can be detected even with flow rate down to 30 L/min. The frequency spectrum of sound signals emitted by water leak is largely within 2 kHz. The comparison of the inside and outside detection approaches is also reported. The leak positioning evaluation proves the feasibility of the leak positioning using the reported MEMS hydrophones. This paper demonstrates a highly efficient, real-time, permanent in-pipe pipeline health monitoring technology based on the MEMS hydrophone sensors. It paves a promising path for water leak detections.

## ACKNOWLEDGMENT

The authors would like to thank Norhanani Jaafar for hydrophone sensor assembly. We also thank Mr. Qingyun Xie at Massachusetts Institute of Technology (MIT) for his valuable discussion in preparing this manuscript.

## REFERENCES

- [1] A. C. McIntosh, *Asian Water Supplies Reaching the Urban Poor*, London, UK: Asian Development Bank, 2003.
- [2] C. Lallana and N. Thyssen, *Water use efficiency (in cities): Leakage*, Copenhagen: European Environment Agency, 2003.
- [3] R. Frauendorfer and R. Liemberger *The issues and challenges of reducing non-revenue water*, London, UK: Asian Development Bank, 2010.
- [4] "Stated NRW (Non-Revenue Water) Rates in Urban Networks", *The Smart Water Networks Forum*, Aug. 2011.
- [5] B. Kingdom, G. Soppe, and J. Sy, "What is non-revenue water? How can we reduce it for better water service?", *The Water Blog*, Aug. 31, 2016. <https://blogs.worldbank.org/water/non-revenue-water-management-has-it-s-time-finally-come>
- [6] L. W. Mays, *Water Distribution Systems Handbook*, New York: McGraw-Hill, 2000.
- [7] O. Hunaidi, W. T. Chu, A. Wang, W. Guan, "Leak detection method for plastic water distribution pipes", *Seminars on Water & Sewer Infrastructure Systems: Challenges and Solutions*, pp. 249-270, Apr. 2000.
- [8] P. Gopalakrishnan, S. Abhishek, R. Ranjith, R. Venkatesh, and V. Jai Suriya, "Smart Pipeline Water Leakage Detection System", *International Journal of Applied Engineering Research*, vol. 12, no. 16, pp. 5559-5564, 2017.
- [9] D. Chatzigeorgiou, A. Khalifa, K. Youcef-Toumi, R. Ben-Mansour, "An in-pipe leak detection sensor: Sensing capabilities and evaluation", *Proc. ASME/IEEE Int. Conf. Mechatron. Embedded Syst. Appl.*, pp. 481-489, Aug. 2011.
- [10] O. Hunaidi, A. Wang, M. Bracken, T. Gambino, and C. Fricke, "Detecting leaks in water-distribution pipes", *Nat. Res. Council Canada Tech. Rep.*, vol. 29, no. 4, pp. 52-55, Jun. 2005.
- [11] Z. Liu and Y. Kleiner, "State-of-the-art review of technologies for pipe structural health monitoring", *IEEE Sensors J.*, vol. 12, no. 6, pp. 1987-1992, Jun. 2012.
- [12] S. P. Siebenaler and G. R. Walter, "Detection of Small Leaks in Liquid Pipelines Utilizing Distributed Temperature Sensing", *Proc. Int. Pipeline Conf.*, Calgary, Canada, Sept. 24-28 2012.
- [13] S. B. Costello, D. N. Chapman, C. D. F. Rogers, and N. Metje, "Underground asset location and condition assessment technologies", *Tunnelling Underground Space Technol.*, vol. 22, no. 5-6, pp. 524-542, Nov. 2007.
- [14] J. Zhang, A. Hoffman, K. Murphy, J. Lewis, and M. Twomey, "Review of pipeline leak detection technologies", *PSIG Annual Meeting. Pipeline Simulation Interest Group*, 2013.
- [15] A. Sadeghiyan, N. Metje, D. Chapman, and C. Anthony, "SmartPipes: Smart Wireless Sensor Networks for Leak Detection in Water Pipelines", *J. Sens. Actuator Networks*, vol. 3, no. 1, pp. 64-78, 2014.
- [16] A. Whittle, M. Allen, A. Preis, and M. Iqbal, "Sensor networks for monitoring and control of water distribution systems", *Proc. 6<sup>th</sup> Conf. Structural Health Monitor. Intell. Infrastruct.*, 2013.
- [17] M. Allen, A. Preis, M. Iqbal, and A. Whittle, "Water Distribution System Monitoring and Decision Support Using a Wireless Sensor Network", *Software Engineering Artificial Intelligence Networking and Parallel/Distributed Computing (SNPD) 2013 14<sup>th</sup> ACIS International Conference on*, pp. 641-646, July 2013.
- [18] G. Q. Wu, J. H. Xu, X. L. Zhang, N. Wang, D. L. Yan, J. L.-K. Lim, Y. Zhu, W. Li, and Y. D. Gu, "Wafer-Level Vacuum-Packaged High Performance AlN-on-SOI Piezoelectric Resonator for Sub-100 MHz Oscillator Applications", *IEEE Trans. Ind. Electron.*, vol. 65, no. 4, pp. 3576-3584, Apr. 2018.
- [19] J. Xu, X. Zhang, S. N. Fernando, K. T. Chai, and Y. Gu, "AlN-on-SOI platform-based micro-machined hydrophone", *Appl. Phys. Lett.*, vol. 109, no. 3, p. 032902, Jul. 2016.
- [20] J. Xu, X. Zhang, S. N. Fernando, S. Merugu, K. T. Chai, and Y. Gu, "AlN-on-SOI platform-based MEMS hydrophone with ultra-low operation frequency and ultra-high noise resolution", *Proc. IEEE MEMS'2016*, Jan. 2016, pp. 1086-1089.
- [21] J. Xu, J. M. Tsai, W. Sun, and C. Sun, "Sensor with vacuum-sealed cavity", *US patent no. US20140230557*, Apr. 26, 2016.
- [22] J. Karki, "Signal conditioning piezoelectric sensors", *Texas Instruments, Application Note SLOA033A*, 2000.
- [23] Y. Khulief, A. Khalifa, R. Mansour, and M. Habib, "Acoustic Detection of Leaks in Water Pipelines using Measurements inside Pipe", *J. Pipeline Syst. Eng.*, vol. 3, no. 2, pp. 47-54, 2012.
- [24] D. Chatzigeorgiou, K. Youcef-Toumi, A. Khalifa, and R. Ben-Mansour, "Analysis and design of an in-pipe system for water leak detection", *Proc. ASME Int. Des. Eng. Tech. Conf. Comput. Inf. Eng. Conf.*, pp. 1007-1016, Aug. 2011.
- [25] Brüel & Kjaer, datasheet, "Hydrophones - Types 8103, 8104, 8105 and 8106", Sep. 2017.
- [26] Benthowave Instrument Inc., product datasheet, available: <https://www.benthowave.com/products/BII-7150Hydrophone.html>.
- [27] DolphinEar Hydrophones, product datasheet, available: <http://www.dolphinear.com/de200.html>.
- [28] Aquarian Audio, datasheet, "H2a Hydrophone User's Guide".
- [29] J. M. Hovem, *Marine Acoustics: The Physics of Sound in Underwater Environments*, Los Altos, California: Peninsula Publishing, 2010.
- [30] L. Zhang, Y. Wu, L. Guo, and P. Cai, "Design and implementation of leak acoustic signal correlator for water pipelines", *Inf. Technol. J.*, vol. 12, no. 11, pp. 2195-2200, 2013.



**Jinghui Xu** received the B.Eng. degree in automatic engineering from Chang'an University, Xi'an, China, in 2003, and the M.S. and Ph.D. degrees in mechanical engineering from Northwestern Polytechnical University, Xi'an, China, in 2006 and 2009, respectively.

From 2009 to 2010, he was a Postdoctoral Researcher with the Department of Microsystems Engineering, Albert Ludwig's Freiburg University, Freiburg, Germany. Since 2010, he has been with Institute of Microelectronics, Agency for Science, Technology and Research (A\*STAR), Singapore, and currently is a Research Scientist. He holds three U.S. patents and completed two times IP licensing. His research interests include acoustic (hydrophone, microphone, pMUT, etc.,) and vibrational MEMS (resonator, oscillator, accelerator, etc.,) based on piezoelectric AlN platform.



**Eva Leong-Ching Wai** received her Bachelor Degree of Materials Engineering from Nanyang Technology University (NTU), Singapore, in 2003. She worked in semiconductor packaging Industrial for two years after graduated from University. Since then, she has been with Institute of Microelectronics, A\*STAR, Singapore, where she is currently the Senior Research Engineer of Interconnect and Packaging Platform.



**Kevin Tshun-Chuan Chai** received the B.Eng. (Hons.) and the Ph.D. degree in electronic and electrical engineering from the University of Glasgow, U.K., in 2002 and 2007 respectively developing tissue cell imaging solution based on Electrical Impedance-Tomography on a CMOS chip.

He joined Institute of Microelectronics, A\*STAR, Singapore in 2008 as a Research Scientist and developed a silicon nanowire based biosensor readout system for the detection of biomarkers in cardiac disease. He has received several competitive A\*STAR grants as PI/Co-PI for MEMS sensor-related applications in temperature, motion and sound detection, cell counting, electronic stethoscope system for the early detection of diastolic dysfunction in hypertensive heart disease etc. He currently heads a department of more than 30 IC designers working on various topics from AI powered hardware accelerators looking at both deep learning and neuromorphic methodologies, compute-in-memory using emerging memories, hardware security for edge IoT, power management solution with IVR, mmWave IC and design acceleration techniques using machine learning.



**Wei Li** received the B.Eng and Ph.D. in microelectronics from Nanyang Technological University, Singapore, in 2005 and 2009, respectively, and the M.B.A. degree from INSEAD, Fontainebleau, France, in 2012. He has many years of experience in technology development, IP management, technology commercialization, start-up incubation and investment. He is currently the General Manager of JCS Venture Lab and founding CEO of CSF Ventures. He is also Adjunct Assistant Professor at Singapore University of Technology and Design (SUTD) for SUTD Technology entrepreneurship program.



**Jason Yeo** received the Diploma of Engineering in Factory Automation from Ngee Ann Polytechnic, Singapore, in 1989 and EMBA from National University of Singapore, Singapore, in 2015. He founded JCS in 1990 and led JCS to become a multinational group company with growing businesses in a range of deep-tech industries. Mr. Yeo is currently the Chairman of JCS Group and JCS Venture Lab. He is also the Chairman of Mclean, a listed company in Malaysia.



**Guoqiang Wu** received the B.Eng. degree in electrical science and technology from Xidian University, Xi'an, China, in 2008, and the Ph.D. degree in microelectronics and solid-state electronics from the Shanghai Institute of Microsystem and Information Technology (SIMIT), Chinese Academy of Sciences, Shanghai, China, in 2013.

He is currently a Research Scientist with the Institute of Microelectronics, Agency for Science, Technology and Research (A\*STAR), Singapore. His research interests include microelectromechanical systems (MEMS) resonators, RF MEMS, inertial MEMS, MEMS integration and packaging technologies.

Dr. Wu was the recipient of the Best Dissertation Award of Shanghai in 2014.



**Edwin Nijhof** has more than 25-years working experience in high tech industry and he has worked in several multinational corporations and startups for their technology development and regional operations. He is currently the Chief Technology Officer of JCS Group, JCS Venture Lab and the General Manager of JCS Technologies.



**Beibei Han** received her B.S. degree in electronic science and technology from Shandong University, China, in 2006, M.S. degree in mechanical engineering from Korea University of Technology and Education, South Korea, in 2008, and her Ph.D. degree in Microelectronics from Nanyang Technological University (NTU), Singapore, in 2015.

From 2008 to 2010 she was a research scientist working on cognitive robotics and simulation at KIST and KAIST. Since 2015, she is a scientist with the Institute of Microelectronics, A\*STAR, Singapore. Her research interest focuses on physical MEMS sensors and acoustic sensor systems.



**Yuandong Gu** received the M.E.E. degree in electrical engineering and the Ph.D. degree in pharmaceutics from the University of Minnesota, Minneapolis, MN, USA, in 2001 and 2003, respectively. He is currently the Deputy Executive Director (DED) in the Institute of Microelectronics, Agency for Science, Technology and Research (A\*STAR), Singapore. Before joining IME, he was a Principal Research Scientist at the Honeywell Sensors and Wireless Lab for ten years.